STRESS AND FAILURE ANALYSIS OF DOUBLE-BOLTED JOINTS IN DOUGLAS-FIR AND SITKA SPRUCE

M. U. Rahman[1]

Research Scientist
Eastman Kodak Co., Rochester, NY 14652

Y. J. Chiang[1]

Assistant Professor
Department of Mechanical Engineering
Detroit University, Detroit, MI 48221

and

R. E. Rowlands

Professor
Department of Engineering Mechanics
University of Wisconsin, Madison, WI 53706

ABSTRACT

Stresses in, and strength of, single- and double-bolted mechanical joints in wood members are analyzed experimentally and numerically. The analyses account for the nonlinear geometric and stress-strain responses and the thicknesses of the members. Stresses are obtained using finite elements, strain gages, and moiré techniques. Failure is predicted from assumed strength criteria. Stresses and strength are influenced by end-distance, bolt-spacing, edge-distance, bolt-clearance, and load distribution between bolts of a multiple fastener. Predicted initiation of failure agrees with visible and audible damage initiation in full-scale components. These occur at 10 to 25% of ultimate structural strength.

Keywords: Bolted joints, mechanical fasteners, finite elements, moiré, strain gages, failure theories, testing, nonlinearity.

INTRODUCTION

Mechanical fasteners are common in timber construction (Fig. 1), but available design information tends to be empirical and available for only simple cases. Development of improved procedures has been inhibited by insufficient knowledge of the stresses in the wood surrounding the bolt-loaded holes. It is typically assumed that connector end distance and bolt spacing are adequate to develop the full strength of each bolt individually (National Forest Products Association 1986). However, in practice space and load requirements often necessitate using multiple fasteners whose end distance and/or bolt spacing is less than sufficient to develop the maximum strength of each bolt individually. Moreover, individual bolts of a multiple-fastener joint do not necessarily load up evenly, and the cosine stress distribution, which is often assumed, is inadequate. In view of the above,
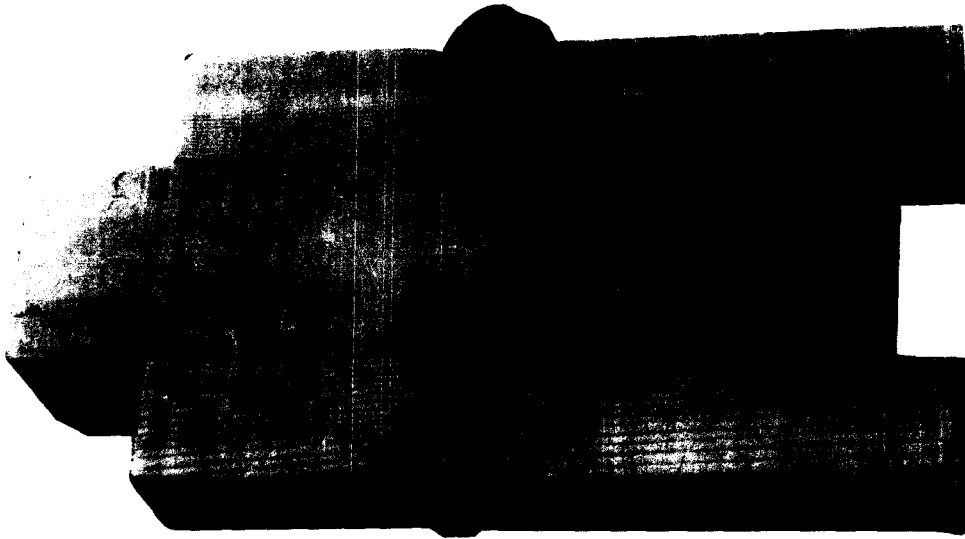

FIG. 1. Cut-away of previously loaded single-bolted fastener in wood.

the stresses and loads at failure initiation of actual mechanical fasteners in Sitka spruce and Douglas-fir are predicted here numerically using finite-elements and strength criteria. Some damage progress is also evaluated. Predicted results are verified experimentally.

Enhanced fastener analysis and design information will help improve structural reliability and facilitate efficient use of wood products. Results herein suggest that the currently recommended end distances may be conservative, the longitudinal bolt spacing of four times the bolt diameter is reasonable, and that the presently recommended minimum bolt clearance should be reduced. Also, the load distribution between individual holes of a multiple-bolt connector can significantly influence the strength and failure mode.

Figure 1 is a photograph of a cut-away of a previously loaded single mechanical fastener in wood, whereas Fig. 2 is a cross section of a double-bolted joint. Bolted joints of this investigation were modeled numerically as shown in Fig. 3. Plane-stress was assumed. The problem is geometrically nonlinear because of the increasing area of bolt contact with increasing load.

Eight-node isoparametric quadrilateral elements, strain gages, high-resolution moiré, and linear and nonlinear stress-strain wood properties were used. Friction at the wood-bolt interface was accounted for, as were bolt clearance and wood compliance between the bolt-loaded holes. Numerically, the bolts were assumed to be rigid. Effects of bolt spacing, end distance, member thickness, and load ratio between the bolts were evaluated. Tsai-Hill, Cowin and Tsai-Wu strength criteria (Rowlands 1985) were employed.

Predicted stresses agree with those determined experimentally. Mode of failure depends on the in-plane geometry of Fig. 3, and the relative loading between fastener bolts. The present numerical model predicts the structural load and location of damage at initial failure. The predicted initiation of fastener failure
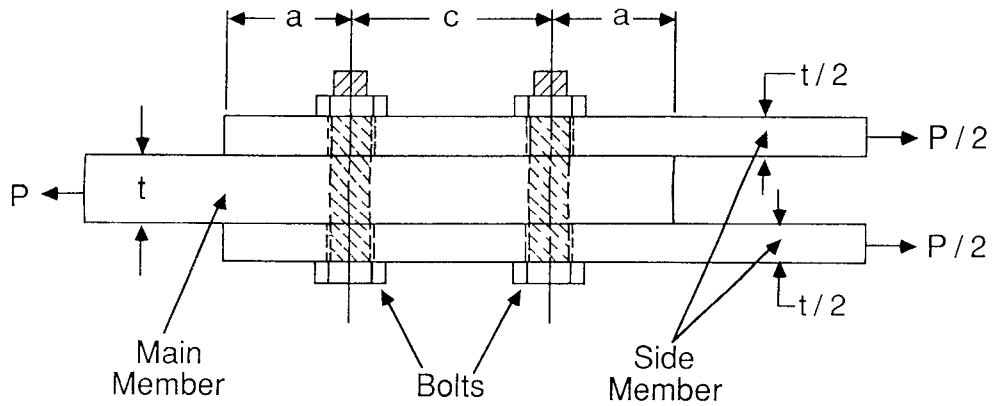
FIG. 2. Cross-section of double-bolted mechanical fastener.

agrees with initial wood failure of the full-scale components, both typically occurring at approximately ten to twenty-five percent of ultimate structural strength.

LIST OF SYMBOLS

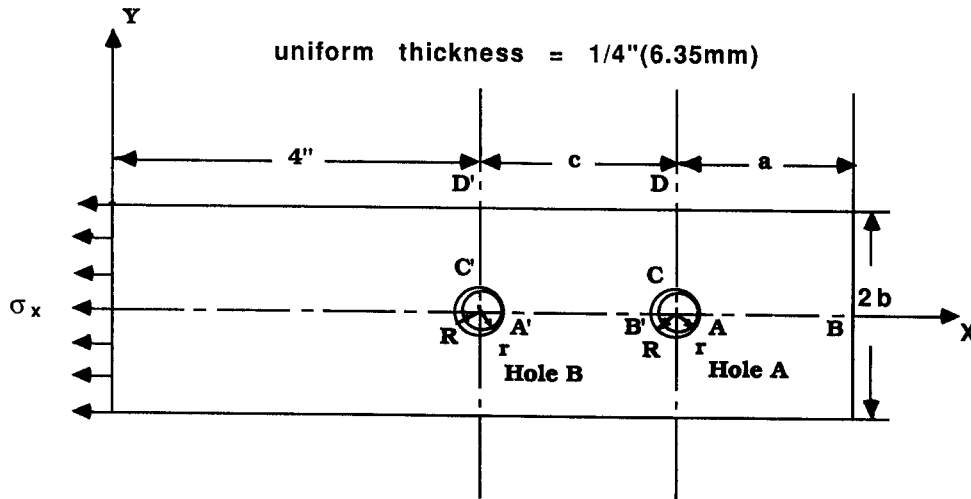|	
a	plate end distance
a_i	polynomial coefficients
b	plate half-width
c	distance between bolts
E_{ii}	Young's moduli
F_i, F_{ij}	strength coefficients
G_{ij}	shear modulus
N	moiré fringe order
P	load

FIG. 3. Schematic of double-bolted mechanical fastener.

p   moiré pitch
P_A load on bolt(hole) A
P_B load on bolt(hole) B
P_A/P_B percent of total load on bolt(hole) A to that on bolt(hole) B
P_{AF} total structural load when failure initiates at hole A
P_{BF} total structural load when failure initiates at hole B
R   hole radius
r   bolt radius
r, θ polar coordinates
S   shear strength
t   main member thickness
u, v   displacements
X   tensile strength parallel to the grain
X' compressive strength parallel to the grain
Y   tensile strength transverse to the grain
Y' compressive strength transverse to the grain
x, y   rectangular coordinates
ξ, η local natural coordinates
μ coefficient of friction
σ, τ stresses
β fringe multiplication number
γ numerical contact tolerance
ν Poisson's ratio
1, 2, 6   material directions as subscripts

RELEVANT PREVIOUS INVESTIGATIONS

Numerous studies of mechanical joints and the associated problem of bolt-loaded holes have been conducted. These include articles by Agarwal (1980); Bodig and Farquhar (1988); Chang et al. (1982); Chiang (1983); Chiang and Rowlands (1987); Cramer (1968); Crews and Naik (1986); Fan (1988); Garbo and Ogonowski (1981); Herrera-Franco and Cloud (1986); Hyer and Liu (1984); McLain and Thangjitham (1983); Oplinger (1976); Oplinger and Gandhi (1974a, b); Patton-Mallory (1988a, b); Prabhakaren (1982); Pyner and Matthews (1979, 1980); Rahman (1981); Rahman et al. (1984); Rahman and Rowlands (1990); Rowlands et al. (1982); Saba et al. (1988); Salinas (1988); Soltis and Wilkinson (1987); Walker and Morrow (1988); Waszczak and Cruse (1971, 1973); Wilkinson et al. (1981); Wilkinson and Rowlands (1981a, b); Wilson and Tsujimoto (1986); and Yen (1978).

Few of the papers on this topic involve wood, and even fewer evaluate actual stresses (or strains) experimentally, impose strength criteria, or consider interactions among bolt-loaded holes. Rahman (1981) combined strength criteria with experimental and numerical stress analyses to predict the strength of bolted joints in wood and fiber-reinforced composites. While experimental stress analyses associated with bolted joints in other orthotropic materials have been conducted by Rowlands et al. (1982), Hyer and Liu (1984), Prabhakaran (1982) and Herrera-Franco and Cloud (1986), only Wilkinson and Rowlands (1981a, b), Rahman (1981) and Chiang (1983) appear to have applied such applications to wood. Little

information exists concerning the effect of member thickness or nonlinear constitutive behavior in bolted joints, although yield models in bolted wood joints were discussed by McLain and Thangjitham (1983). Cramer (1968), Garbo and Organowski (1981), Yen (1978) and Herrera-Franco and Cloud (1986) have considered multiple-bolt connectors, but Rahman (1981) appears to be the first to actually stress (experimental-numerical) analyze this important case. End effects under tensile and compressive loading were compared by Patton-Mallory (1988a), and the response of loading transverse to the grain was reported by Walker and Morrow (1988). Bodig and Farquhar (1988) evaluated the effects of accelerated strain rates, while reliability bounds and a connector optimization procedure were proposed by Salinas (1988) and Saba et al. (1988). Unfortunately, the latter approach appears to ignore important effects such as relative bolt clearance. Patton-Mallory (1986b) described acoustic emission monitoring of the damage progress in a loaded bolted joint in wood, and Chiang and Rowlands (1987) studied the crack propagation eminating from bolt-loaded holes.

FINITE-ELEMENT ANALYSIS

It is important numerically to account for bolt clearance, fixation and sliding friction between the bolt and contacting wood, and the compliance between bolt holes of multiple-bolt connectors. Our finite-element approach for bolted joints in wood has progressed through several stages. With single-fastener joints, we initially assumed a linear stress-strain wood response and employed iteration to maintain contacting nodes of the wood virtually on the surface of the loading bolt (Wilkinson et al. 1981; Wilkinson and Rowlands 1981a, b). Rectangular coordinates and a stationary bolt were used, and the wood was "pulled around the bolt."

For double-bolted mechanical fasteners such as those of Figs. 2 and 3, Rowlands et al. (1982), Rahman et al. (1984) and Rahman and Rowlands (1990) used a global set of rectangular coordinates, as well as a local set of rectangular and polar coordinates at each bolt-hole whose origins were at the center of the respective bolt. This enables one to account for the compliance between bolt holes and permits the contacting nodes of the wood to be maintained on the surface of a loading bolt. Compared to our earlier numerical scheme described in the previous paragraph, this present method eliminates the partial unloading iterations needed previously to maintain contacting nodes on a bolt. It also satisfies the contact and friction conditions more accurately, has the numerical advantage of being more modular, and provides accurate analysis with fewer elements. The ability to use fewer elements is particularly significant with multiple-bolt fasteners. Computer analyses of a multiple-bolt fastener are already time-consuming because friction (determining regions of slip and fixation conditions) and the desire to achieve a particular load-ratio between individual bolts necessitate separate iterative procedures.

The previous finite-element method by Wilkinson et al. (1981) for a single bolt pulled the wood around a stationary bolt. In the present approach by Rahman and Rowlands (1990), the wood is held stationary at the left end of Fig. 3, and each of the bolts is moved incrementally into the wood using an iterative scheme to maintain the desired loading ratio between bolts.

The following load-ratios (percent) have been considered between individual bolts of multiple-bolt fasteners, Rahman (1981): P_A/P_B = 0/100, 30/70, 50/50, 70/30, and 100/0. P_A is the load on bolt A, while P_B is the load on bolt B (Fig. 3). Some of the load ratios were studied under varying distance c between bolt holes. Unless stated otherwise, width 2b = 3 in. (7.62 cm) and thickness t = 0.25 in. (0.635 cm). Cases are considered presently for each of end distance a = 1 in., 2 in. and 3 in. (2.54 cm, 5.08 cm and 7.62 cm). Space permits presenting only limited results here. The reader is directed to the theses by Rahman (1981) and Chiang (1983) for additional information and details.

Many wood species have nonlinear stress-strain responses, particularly in compression. The above finite-element scheme was subsequently modified here to incorporate nonlinear stress-strain behavior of the wood. This was accomplished using tangent moduli (Chiang 1983).

Curved isoparametric quadrilateral elements having eight nodes and 16 degrees of freedom were used. The interpolation polynomial for the displacements of this element is of the following form:

$$u(\xi, \eta) = a_1 + a_2\xi + a_3\eta + a_4\xi^2 + a_5\xi\eta + a_6\eta^2 + a_7\xi^2\eta + a_8\xi\eta^2. \tag{1}$$

ξ and η are natural coordinates and a_1 are coefficients.

Coulomb friction is assumed between a steel bolt and the wood, and regions of slip and fixation are provided. A contacting node of the wood is fixed to the bolt surface if

$$0 \leq |\mu\sigma_r| - |\tau_{r\theta}| < \gamma. \tag{2}$$

A contacting node continues to slide on the surface of a bolt if

$$|\mu\sigma_r| < |\tau_{r\theta}| \tag{3}$$

where σ_r, $\tau_{r\theta}$ are the radial normal and shear stresses in the wood, and μ = 0.7 (Wood Handbook 1974) is the coefficient of friction. γ is a selected tolerance, and experience demonstrated that values of γ in the range of 1 to 5 psi (6.9 to 34.5 KPa) are suitable.

Current analyses are limited to cases in which the material axes of symmetry are parallel and perpendicular to the geometric and loading axes of symmetry. Symmetry permits modeling numerically half of the joint (Fig. 4). One-half of a plate with end distance a = 2 in., half width b = 1 in. and a single bolt is represented typically by 53 elements and 252 nodes (Rahman 1981). Numerical details for stress analyzing single bolt-loaded members are described by Wilkinson et al. (1981) and Wilkinson and Rowlands (1981a, b), while those for double-bolted joints are discussed by Rahman and Rowlands (1990). For simplicity, the mesh of Fig. 4 is for a single bolt-loaded hole. That for a double bolt-loaded hole consists essentially of repeating the mesh to the right of line HI of Fig. 4 to the right of line JK.

MOIRÉ

Moiré is an optical phenomenon observed when two closely spaced arrays of lines or patterns are superimposed and viewed with transmitted or reflected light. If the two arrays differ in spacing or orientation, interference between the arrays
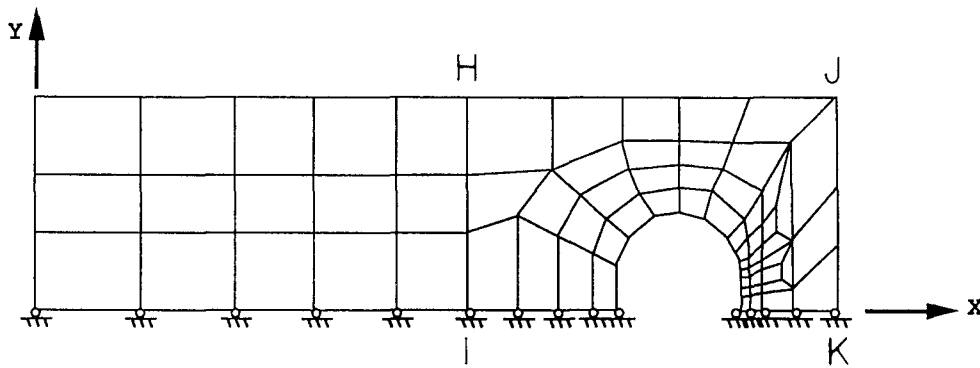
FIG. 4. Finite-element mesh.

produces moiré fringes. In engineering practice, a line array is typically photo-printed or etched onto the surface of the structure whose stresses (strains) are sought. This ruling becomes the active array in that it follows the surface deformations of the loaded structure. A transparent reference or analyzing array is traditionally placed in contact with the active structural array, and the two arrays are aligned and viewed. Although not necessary, one normally uses parallel lines having a common pitch p (1/p = lines/in. or lines/mm) for the active and analyzing grids. As the structure is loaded, the pitch and orientation of its lines change to produce moiré fringes between the active deformed structural ruling and that of the passive analyzer. These fringes can be interpreted in terms of the relative motion between the ruling arrays.

Moiré fringes represent loci of points of constant displacement. The component of the displacement is that transverse to the direction of the analyzing grid. The magnitude of the displacement u is

$$u = Np \qquad (4)$$

where N is the fringe order. Orthogonal rulings may be used to give both u and v components of displacements. Strains are obtained by differentiating the displacements. The stresses can then be obtained from the stress-strain relationship.

Conventional moiré can be insufficiently sensitive. For this reason we employed moiré fringe-multiplication (Post and MacLaughlin 1971; Rahman 1981; Chiang 1983). Instead of forming the moiré fringes in situ by maintaining the active and analyzing arrays in contact during loading of the structure, optical replicas of the deformed active array were recorded photographically on glass plates. These replicas were subsequently analyzed in collimated monochromatic light in series with a blazed reference (analyzing) grating. The frequency of the lines of this blazed analyzing-ruling was an interger multiple β of the undeformed specimen ruling frequency. The resulting moiré fringes correspond to those that would occur had both the active and analyzing rulings been of the dense frequency of the latter. This produces a fringe multiplication of β.

Cross-grids were used for the active array. By sequentially rotating the replicas through 90°, both u and v displacement fringes were obtained from a unidirectional blazed ruling. We used active grids of 500 dots/in. (20 dots/mm) on the wood

TABLE 1. *Measured elastic and strength properties of Sitka spruce and Douglas-fir (Rahman 1981).*

Property	Sitka spruce (psi)	Douglas-fir (psi)
E_x	2.4×10^6	1.7×10^6
E_y	1.2×10^5	0.9×10^5
ν_{xy}	0.5	0.5
G_{xy}	1.4×10^5	1.2×10^5
X	13,000	12,000
X'	5,160	5,000
Y	370	340
Y'	580	500
S	1,150	1,100

and a blazed analyzer of essentially 5,000 lines/in. (200 ℓpmm) to give a fringe multiplication of $\beta = 10$.

STRENGTH CRITERIA

One must have a criterion on which to base a design. This is typically accomplished by formulating some characteristic or limiting stress, strain, or energy condition such that once that limit is reached at any location, failure or damage initiates at that location. Localized failure does not necessarily mean the component cannot continue to carry the applied, or even a higher, load. To predict ultimate strength of a structure requires modeling any damage, or perhaps the unloading of a damaged region.

The Tsai-Hill, Tsai-Wu and Cowin failure theories are used here (Rowlands 1985). These theories are as follows:

● Tsai-Hill

$$\left(\frac{\sigma_x}{X}\right)^2 + \left(\frac{\sigma_y}{Y}\right)^2 - \left(\frac{\sigma_x\sigma_y}{X^2}\right) + \left(\frac{\tau_{xy}}{S}\right)^2 < 1, \tag{5}$$

where X, Y and S are the strengths parallel and perpendicular to the grain, and in shear, respectively.

● Tsai-Wu

$$F_1\sigma_x + F_2\sigma_y + 2F_{12}\sigma_x\sigma_y + F_{11}\sigma_x^2 + F_{22}\sigma_y^2 + F_{66}\tau_{xy}^2 < 1, \tag{6}$$

where:

$$F_1 = \frac{1}{X} - \frac{1}{X'}, \qquad F_2 = \frac{1}{Y} - \frac{1}{Y'},$$

$$F_{11} = \frac{1}{XX'}, \qquad F_{22} = \frac{1}{YY'},$$

$$F_{66} = \frac{1}{S^2}, \qquad F_{12} \leq \sqrt{F_{11}F_{22}}, \tag{7}$$

and primed values denote compressive strengths. F_{12} was taken here to be zero.
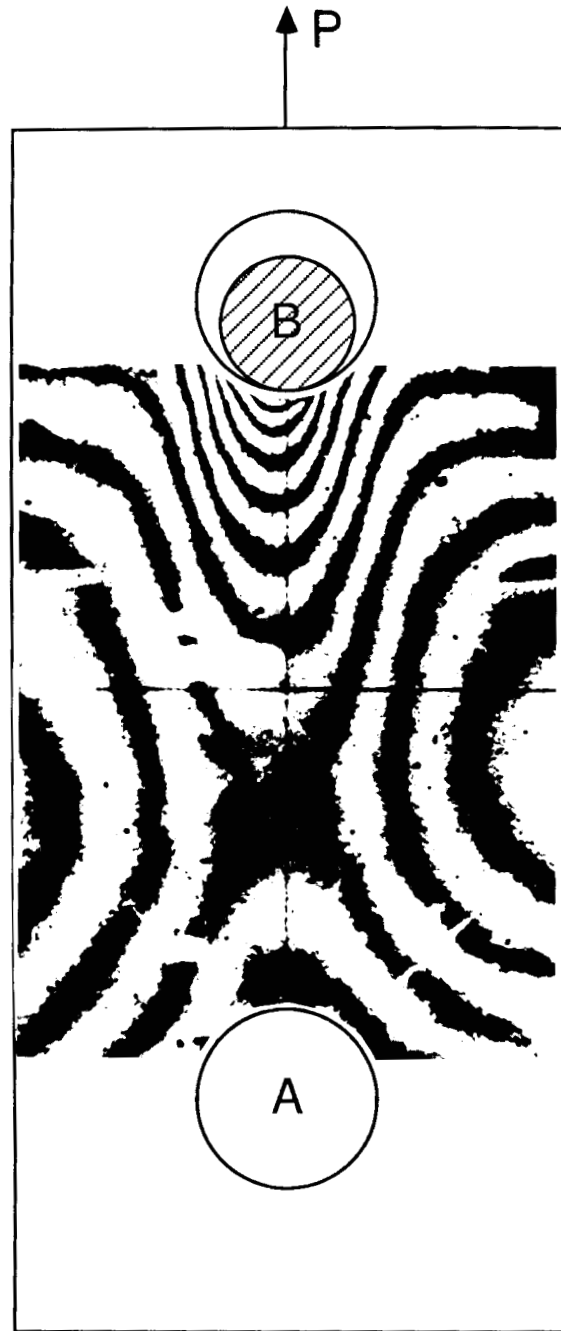
FIG. 5. Moiré fringe pattern of the vertical displacements between holes of a double-bolted mechanical fastener in Sitka spruce: $(P_A/P_B) = 00/100$, $P = 100$ lb, a = 1 in., b = 1.5 in., c = 2 in., t = 0.25 in., R = 0.25 in., r/R = 0.924; 5,000 ℓpi Equivalent.
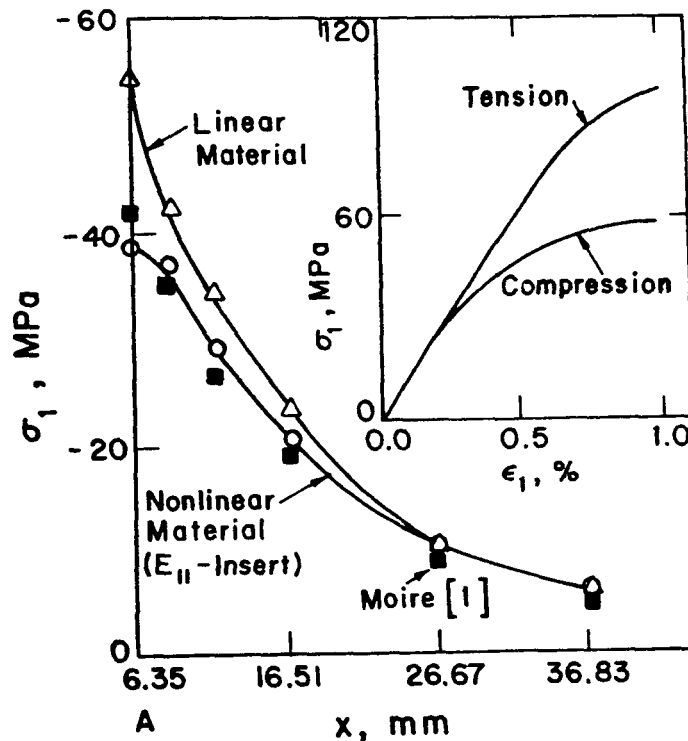
Fig. 6. Effect of material nonlinearity of spruce on longitudinal stress σ_1 along line AB of a single-fastener bolted joint. (a = 3 in., b = 1.5 in., t = 0.25 in., R = 0.25 in., r/R = 0.936, P = 250 lb, E_{22} = 82 ksi, ν_{12} = 0.5, G_{12} = 95 ksi).

● Cowin

Same as the Tsai-Wu theory except

$$F_{12} = \sqrt{F_{11}F_{22}} - \frac{1}{2S^2}.$$ (8)

Measured elastic and strength properties of Sitka spruce and Douglas-fir are shown in Table 1. The wood was conditioned at 65% RH and 74 F to maintain a moisture content of 12%. The article by Rowlands (1985) reviews anisotropic biaxial strength theories, including those used for wood.

RESULTS

Experimental-numerical stress correlation

Parametric studies are most conveniently conducted numerically, but the complexity of the finite-element analysis warranted experimental verification. Figure 5 is a typical photograph of the moiré fringes between bolt holes of a double-bolted connector in Sitka spruce. The bottom hole of this pattern is unloaded. Fringes represent loci of points of equal vertical displacement in 0.0002 in. (0.005 mm) increments. Figure 6 and the articles by Wilkinson and Rowlands (1981a,

TABLE 2. *Stress beneath loading bolts in Sitka spruce from strain gages and finite elements:* $P_A + P_B = 100$ *and 200 lb;* $P_A/P_B = 100/00$ *and* $00/100$ ($t = 0.25$ in., $R = 0.25$ in., $r/R = 0.924$, $a = 3$ in., $b = 1.5$ in.).

Hole A				
x distance	Stress, σ_v, for $P_A + P_B = 200$ lb $P_A/P_B = 100/00$		Stress, σ_v, for $P_A + P_B = 100$ lb $P_A/P_B = 100/00$	
	Strain gages	Finite element	Strain gages	Finite element
6.47"	$-1,920$ psi	$-2,181$ psi	$-1,346$ psi	$-1,126$ psi
6.80"	$-1,403$ psi	$-1,236$ psi	-729 psi	-631 psi

Hole B				
x distance	$P_A + P_B = 200$ lb $P_A/P_B = 00/100$		$P_A + P_B = 100$ lb $P_A/P_B = 00/100$	
	Strain gages	Finite element	Strain gages	Finite element
4.47"	$-1,609$ psi	$-2,133$ psi	-790 psi	$-1,099$ psi
4.80"	$-1,109$ psi	$-1,154$ psi	-535 psi	-590 psi

b), Rahman (1981) and Chiang (1983) contain further moiré and finite-elements correlations for bolted connections.

Some Sitka-spruce specimens were also instrumented with electrical resistance strain gages. These specimens were 0.25 in. (6.35 mm) thick, end distance a = 3 in. (7.62 cm), 2R = 0.50 in. (12.7 mm), and 2r = 0.462 in. (11.73 mm) so r/R = 0.924. Strain gages were located along lines AB, A'B', CD and C'D' of Fig. 3. Table 2 contains representative results. Articles by Wilkinson and Rowlands (1981a) and Rahman (1981) contain additional strain gage results.

Geometric effects

The maximum radial contact stress in the wood increases with increased bolt clearance. Also, the maximum radial contact stress can occur at locations other than directly under the bolt, and a serious transverse tensile stress is produced at location B of Fig. 3, as the end-distance a is reduced. Such aspects have been demonstrated previously for single-bolted wood connectors by Wilkinson and Rowlands (1981a). The effect of end distance on the radial stress beneath the contacting bolts of a double-fastener joint is shown in Figs. 7 and 8. Bolt spacing is c = 2 in. (5.08 cm), the bolt holes are equally loaded ($P_A/P_B = 50/50$), end distance a = 1 in. (2.54 cm) and 3 in. (7.62 cm), and results are for total load $P_A + P_B = 200(890N)$, 400(1780N) and 800(3560N) pounds, respectively. Figures 7 and 8 illustrate the following features:

1. The radial contact stress does not increase linearly with applied load because increased loading increases the contact area.
2. Reducing the end-distance a such that the structural stiffness supporting bolt A becomes appreciably less than that supporting bolt B reduces the maximum radial stress beneath bolt A, although the stress spreads out.

Reduced structural stiffness supporting a bolt enables the wood to wrap around the bolt. This has a tendency to reduce the maximum contact radial stress, while spreading the stress out. This effect was also noted previously by Wilkinson and Rowlands (1981a, b). The structural stiffness supporting a bolt can decrease either by reducing the amount of material through shortening the end distance, or by
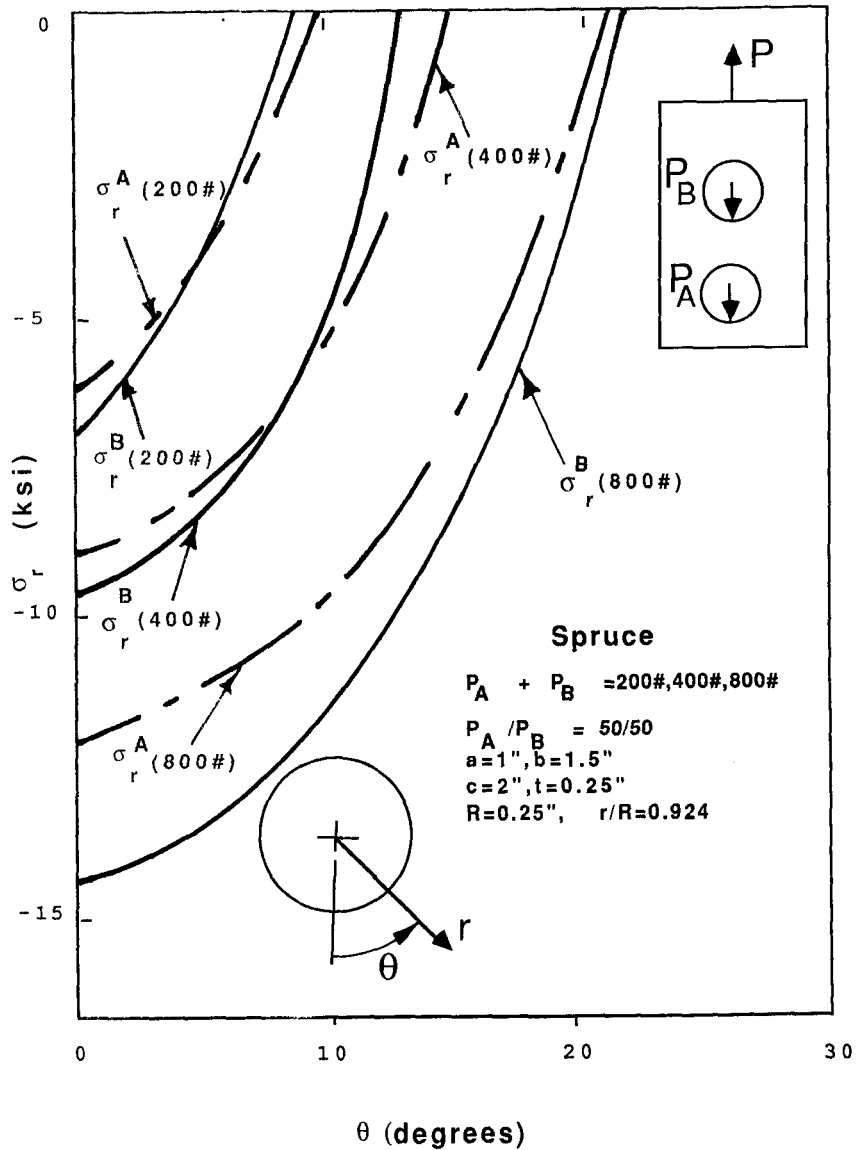
FIG. 7.   Numerically predicted stress σ_r at bolt-loaded holes in Sitka spruce for P_A/P_B = 50/50 and a = 1 in.

employing a more compliant material. A more compliant material is often also weaker. Reducing the end distance can produce excessively high tensile stresses at point B of Fig. 3. Figure 9 shows the increased contact radial stress distribution for a double-bolted joint when only one of the bolts contacts the wood. However, Figs. 7 and 9 show that for identical geometry and total load, the maximum radial contact stress for a single loading bolt is considerably less than twice that for two loading bolts.

Figure 10 illustrates the change in tangential stress around the boundary of hole
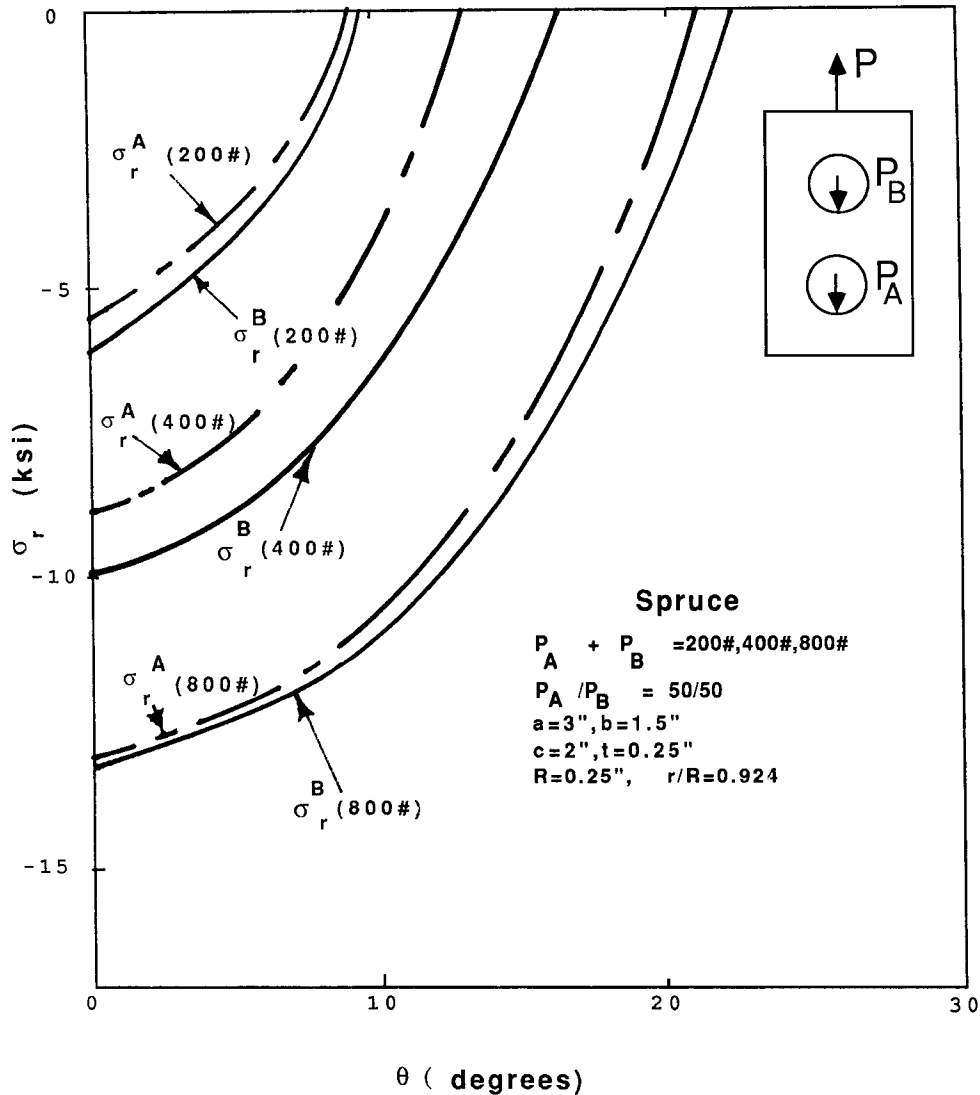
FIG. 8. Numerically predicted stress σ_r at bolt-loaded holes in Sitka spruce for $P_A/P_B = 50/50$ and a = 3 in.

B for a connector of spruce having geometry of Fig. 3 (P = 800lb, 3560N) resisted only by a bolt at A and for hole spacings of c = 2 in. (5.08 cm), 2.5 in. (6.35 cm) and 3 in. (7.62 cm), respectively. The tangential stress at θ = 90° (θ measured from point A' of Fig. 3) on the boundary of unloaded hole B increases with decreasing hole spacing, but the compressive stress at θ = 0° and 180° remains essentially independent of the variations in hole spacing considered. At least for this case, varying the hole spacing over the range 8 ≤ c/R ≤ 12 has little effect on the stresses at hole B. Further studies are warranted for other materials, and loading of both holes when c/R < 8.
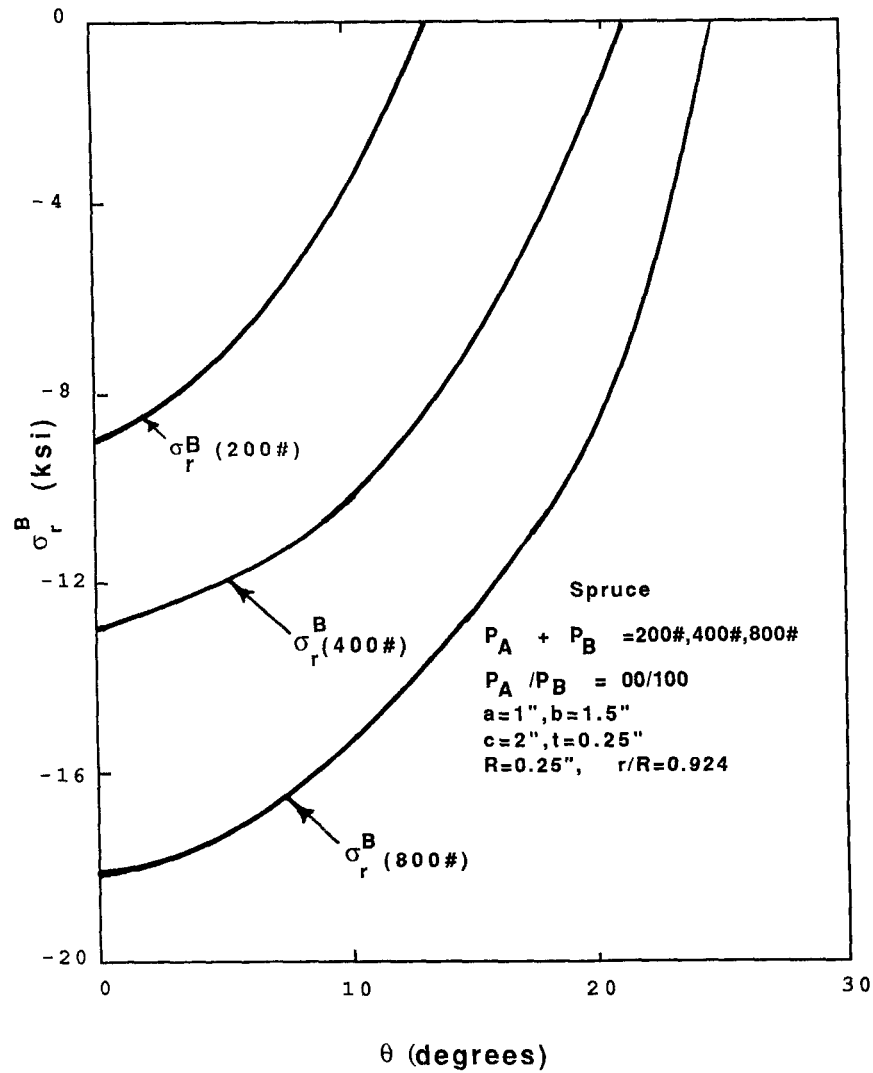
Fig. 9. Numerically predicted stress $\sigma_r{}^B$ at bolt-loaded hole B in Sitka spruce for $P_A/P_B = 00/100$ and $a = 1$ in.

Material nonlinearity

Stress-strain response in wood is often not linear to failure. Figure 6 illustrates material nonlinearity (insert of Fig. 6) for spruce and its effect on the stress beneath a single bolt-loaded hole in a tensile plate. The radial stress at point A on the hole boundary of Fig. 6 is reduced by 20% because of material nonlinearity. Such differences in the stress below a bolt can change the mode of failure beneath the bolt.

Strength

Figure 11 shows the measured ultimate strength of loaded spruce plates of the geometry of Fig. 3. End distance $a = 1$ in. (2.54 cm), 2 in. (5.08 cm) and 3 in.
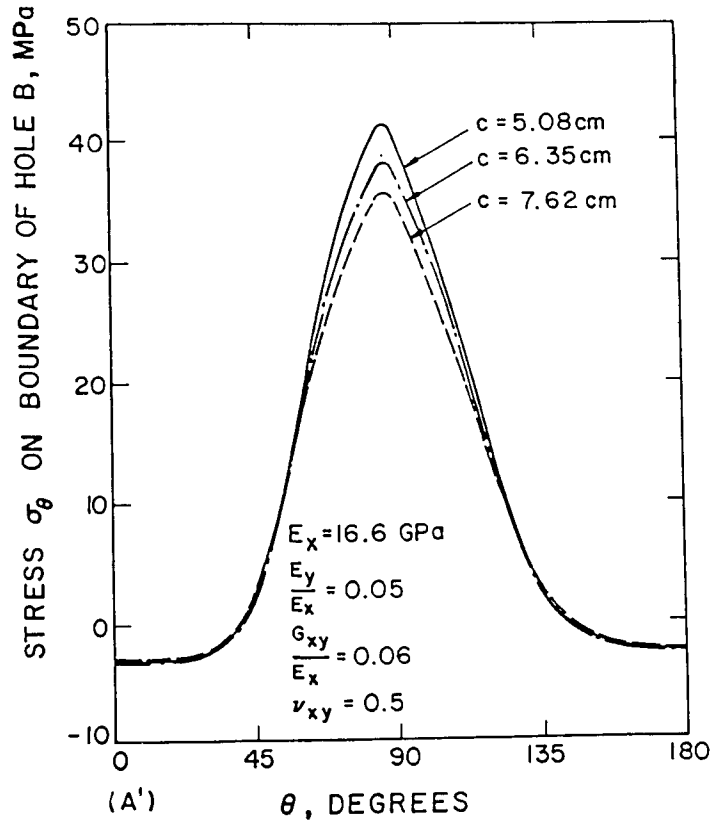
FIG. 10. Effect of hole spacing on the numerically predicted tangential stress at hole B for bolt-loading at hole A only in Sitka spruce (a = 1 in., b = 1.5 in., t = 0.25 in., P = 800 lb, P_A/P_B = 100/00, R = 0.25 in., r/R = 0.924).

(7.62 cm), respectively. Hole A and hole B were bolt-loaded individually in the percent load-ratios of P_A/P_B = 00/100 and P_A/P_B = 100/00, respectively. For a < 2 in., strength is quite dependent on end distance. It is also very significant which hole is loaded. The greater sensitivity to short end distances (a < 2 in. = 5.08 cm) for connector loading P_A/P_B = 100/00 is compatible with the stress profiles of Figs. 7 through 9.

Three-member connectors of Douglas-fir were loaded to failure (Fig. 12). These mechanical connectors were of the geometry of Figs. 2 and 3 with b = 1.5 in. (3.8 cm), c = 2 in. (5.08 cm), hole radius R = 0.25 in. (0.635 cm) and bolt-to-hole ratio r/R = 0.924. End distances were a = 1 in. (2.54 cm) and a = 2 in. (5.08 cm), and central-member thickness t = ½ in. (1.27 cm) and t = 1.5 in. (3.8 cm), respectively. In all cases, the Douglas-fir side members each had a thickness equal to t/2. Regular mild-steel bolts were employed. Flat washers were used on both sides and the nuts were thumb tightened. During specimen preparation, the three members of a double-bolted assembly were drilled as a unit to ensure hole alignment such that both bolts would contact the wood simultaneously when loading the component. Because both the central member and side members of a particular
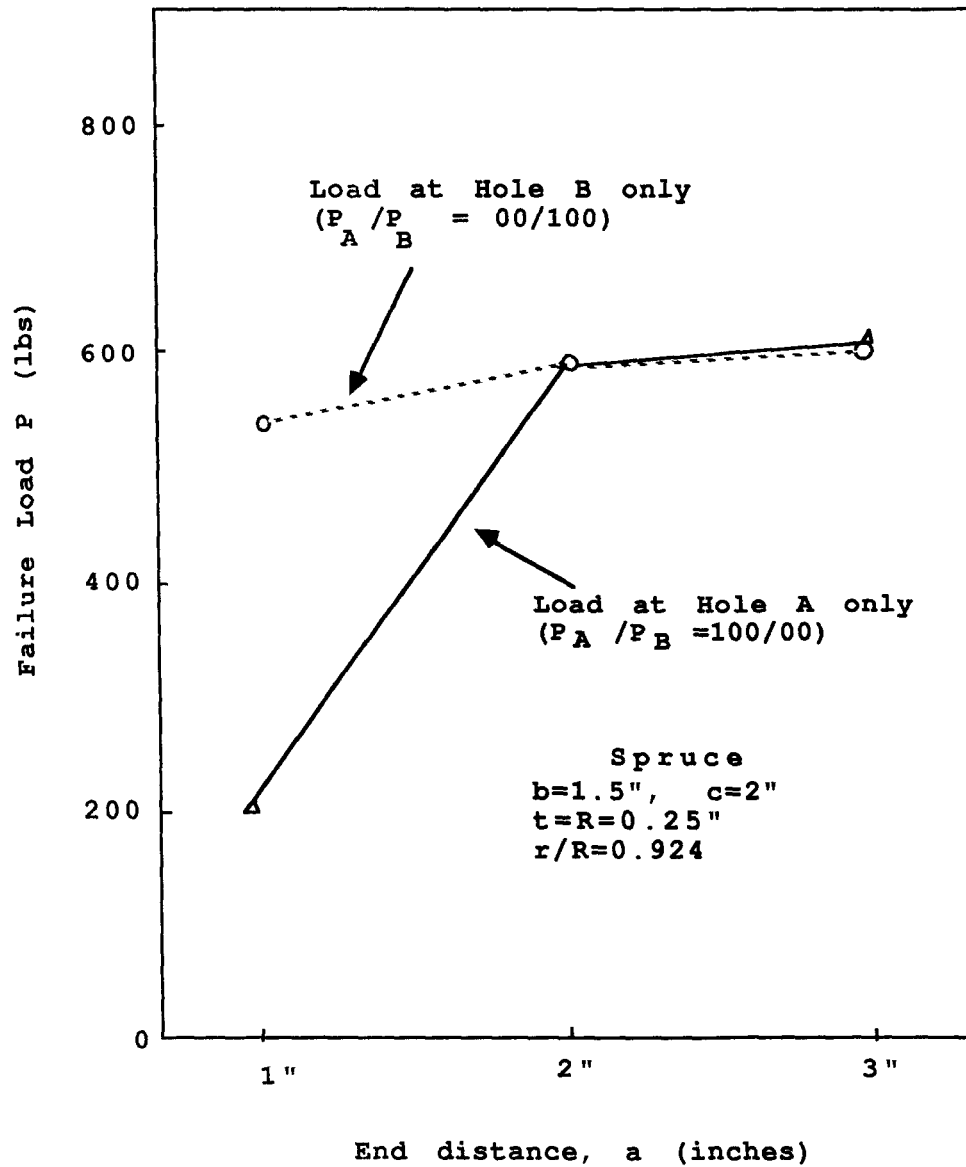
FIG. 11. Measured ultimate strength of Sitka spruce at P_A/P_B = 00/100 and 100/00 and for various end distances (b = 1.5 in., c = 2 in., t = R = 0.25 in., r/R = 0.924).

joint had identical end-distance a, and because the total thickness of the two side members equals that of the central member, the two bolts of such a fastener should, theoretically, load equally. Test results of these three-member, double-fastener bolted joints are contained in Table 3, as are the data of Fig. 11 for some Sitka-spruce tensile plates (t = 0.25 in., b = 1.5 in.) loaded through only one of the two holes (R = 0.250 in. and r/R = 0.924). The Douglas-fir data of each case of Table 3 represent the results of at least five specimens.
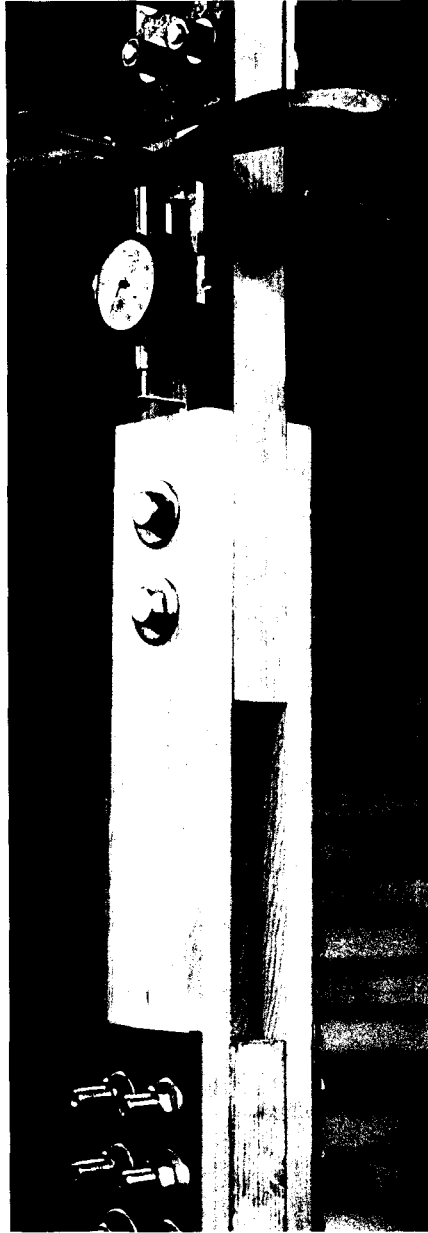
FIG. 12.   Full-scale testing of double-bolted, three-member Douglas-fir mechanical fasteners (b = 1.5 in., c = 2 in., R = 0.25 in., r/R = 0.924).

The National Design Specification for Wood Construction (National Forest Products Assoc. 1986) manual recommends $\dfrac{c}{R} \geq 8$ in order that each bolt carry its full loads; indeed, Fig. 11 indicates such occurs here. The measured strengths of 2,578 lb and 4,950 lb of the three-member fir connectors at t = 1½ in. of Table

(a)   Opening at free end

(b)   Bearing failure

(c)   Cracking and plug failure at free end

(d)   Crack and plug failure at interior hole

FIG. 13. Failure modes in Sitka spruce and Douglas-fir.

TABLE 3. *Measured ultimate strength of three-member double-bolted connectors of Douglas-fir and single plates of Sitka spruce (b = 1.5 in., c = 2 in., R = 0.25 in., r/R = 0.924).*

	Three-member fir joints $P_A/P_B = 50/50$				Single plates of Sitka spruce	
	t = ½ in.		t = 1½ in.		$P_A/P_B = 100/00$	$P_A/P_B = 00/100$
	(Central Member Thickness)					
End distance, a	Load	SD*	Load	SD*	t = 0.25 in.	
1 in.	920 lb	24.5	2,578 lb	268	247 lb	576 lb
2 in.	—	—	4,950 lb	578	583 lb	583 lb
3 in.	—	—	—	—	640 lb	640 lb

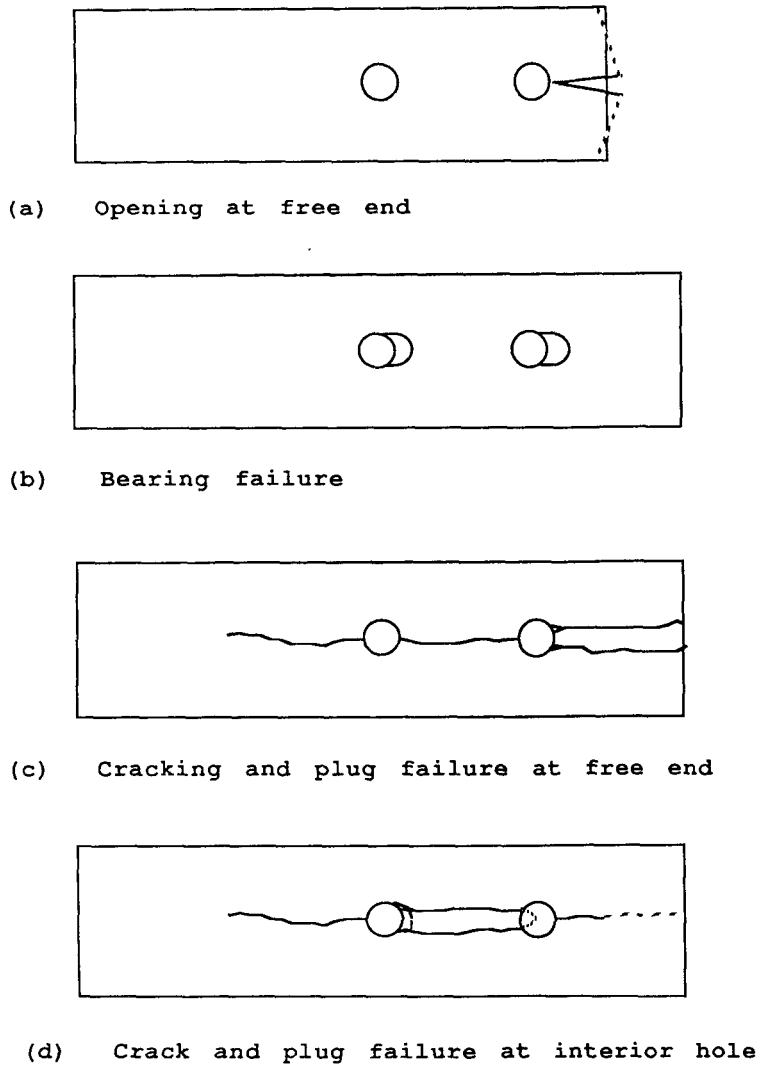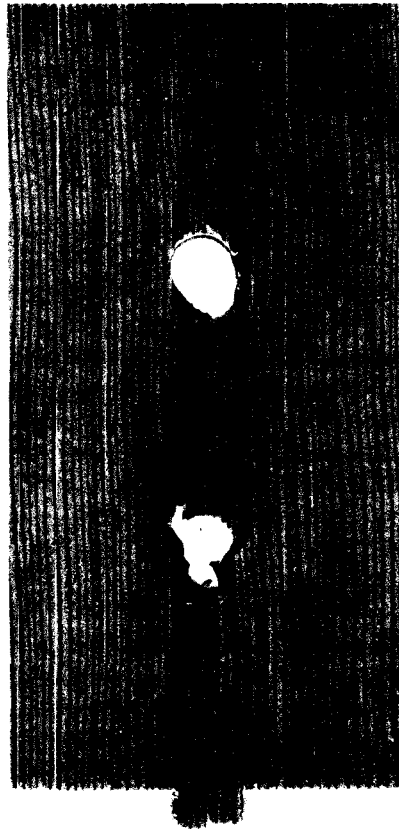* Standard deviation in pounds (minimum of five specimens each).

Fig. 14.   Photograph of failure of three-member double-bolted mechanical fastener in Douglas-fir (a = 2 in., b = 1.5 in., c = 2 in., R = 0.25 in., r/R = 0.924, t = 0.5 in., P_A/P_B = 50/50).

3 well exceed the recommended design value of 2 × 940 = 1,880 lb. This is despite the fact $\frac{a}{R} \leq 8$, which is well below the value of $\frac{a}{R} \geq 14$ recommended for softwoods by the National Design Specifications.

Table 4.   *Total loads* (P_{BF}/P_{AF}) *in pounds at which initial failure is predicted numerically by different failure theories for two end distances (a = 1 in. and 2 in.) in Sitka spruce and Douglas fir at* P_A/P_B = 50/50 *under pin A* (P_{AF}) *and pin B* (P_{BF}); *c = 2 in., b = 1.5 in., R = 0.25 in., r/R = 0.924.*

	Tsai-Hill	Tsai-Wu	Cowin
Douglas-fir* (Based on main member thickness of t = ¼ in.)			
a = 1 in.	80/80	80/80	80/80
a = 2 in.	80/80	80/80	80/80
Sitka spruce (t = ¼ in.)			
a = 1 in.	100/80	100/80	100/80
a = 2 in.	80/100	80/100	50/100

* Correspond to three-member double-bolted fasteners of Table 3.

TABLE 5. *Numerically predicted load to initiate failure in multiple fastener of Sitka spruce under $P_A/P_B = 100/00$ (a = 3 in., b = 1.5 in., c = 2 in., R = t = 0.25 in., r/R = 0.924).*

Criterion	Total load (lb)
Tsai-Hill	50
Tsai-Wu	40
Cowin	50

Some typical failure modes that occurred during testing of the Douglas-fir and Sitka-spruce specimens of Table 3 are shown in Fig. 13. Most of the double-bolted wood joints failed according to Figs. 13(c) or 13(d). However, some bearing failures were exhibited for longer end distances, (Fig. 13(b)). Initial damage was normally observed by about 10-25% of ultimate load. Wood members having end distance a = 1 in. (2.54 cm) often failed by opening at the free end (Fig. 13(a)). Failure of the type shown in Fig. 13(a) was not observed for end distances a $\geq$ 2 in. Figure 14 is a photograph of failure in a failed member of one of the three-member Douglas-fir connectors.

Predicted damage and failure

The failure criteria discussed previously were combined with the numerical stress analysis to predict the type of initial failure and the load at which that occurs. In this case the wood was assumed to respond linear-elastically to failure. Table 4 contains the predicted loads at the initiation of failure for different end distances, load ratio $P_A/P_B = 50/50$ and for two different materials (Douglas-fir and Sitka spruce). All predicted failure loads are based on t = 0.25 in. (0.635 cm). During incremental numerical loading of a connector, the strength theories were evaluated at each load step along hole boundaries AC and A'C' and lines AB and A'B' of Fig. 3.

Table 4 contains the loads (P_{BF}/P_{AF}) at which initial failure was predicted numerically by the different strength theories based on the wood material properties of Table 1. All failures of Table 4 are predicted to start immediately beneath a loaded bolt. P_{BF} represents the total specimen load during initial failure at hole B, whereas P_{AF} represents the total specimen load at initial failure at hole A. For Douglas-fir, initial damage is predicted at 10 to 20% of the total ultimate strength of the three-member connectors of Table 3. Initial damage of the full-size three-member connectors was frequently audible and/or visible by 25% of ultimate load.

Damage is predicted to initiate at a single or several points at loads considerably below the measured ultimate strength. The spruce plates (t = 0.25 in., b = 1.5

TABLE 6. *Numerically predicted extend of progress of failure along curve AC ($\pm\theta$, degrees) and line AB at P = 400 lb in multiple fastener of Sitka spruce under $P_A/P_B = 100/00$ (a = 3 in., b = 1.5 in., c = 2 in., R = 0.25 in., r/R = 0.924, t = 0.25 in.).*

Strength criterion	Curve AC ($\pm\theta$)	Line AB (x)
Tsai-Hill	19°	6.4 in.
Tsai-Wu	19°	6.4 in.
Cowin	19°	6.4 in.

in., c = 2 in., R = 0.25 in., r/R = 0.924) of Table 3 with end distance a = 3 in. (7.62 cm) failed at P = 640 pounds (2.8 kN) when loaded only by bolt A. Table 5 predicts the load to initiate damage for this case, while Table 6 predicts the extent of damage of such a loaded Sitka-spruce plate for P_A = 400 lbs (1780N). Damage is predicted to initiate at point A (θ = 0, x = 6.25 in.), and Table 6 contains only the damage along the contacting surface AC ($\pm\theta$) and its depth of penetration along line AB from location A. Distance x is measured from the left end of Fig. 3. Data of Table 6 must be interpreted cautiously since no progressive wood damage is accounted for numerically once failure is predicted to initiate. Additional results on bolted joints in wood, including use of additional failure criteria, are described by Rahman (1981) and Chiang (1983).

SUMMARY, CONCLUSIONS AND DISCUSSION

Stress and strength analyses of single- and double-bolted mechanical connectors in Douglas-fir and Sitka spruce have been determined numerically and experimentally. Stresses are predicted using finite-elements and are measured by moiré and strain gages. Tsai-Hill, Tsai-Wu and Cowin strength criteria are combined with the stress analysis to predict initial connector failure. The study accounts for the effects of end-distance, bolt-spacing, bolt-clearance, member-thickness, friction (sliding and fixation), and distribution of the loading between bolts. Nonlinear wood properties reduce the contact normal stress by 20% relative to that based on linear elasticity. Full-scale Douglas-fir connectors were tested to failure.

Component failure is predicted to initiate at 10–25% of the ultimate strength. This correlates with the physically observed and/or audible initiation of damage. Failure is predicted here always to initiate immediately below a contacting bolt. For a/R < 8, structural strength is highly influenced by transverse tensile stress at the far end of the wood beneath the end bolt. This is accompanied by relatively low connector strength. Stress distributions in a double-bolted fastener are affected by load distribution among the bolts. Indeed, connector strength is highly influenced by load distribution between the bolts for $\frac{a}{R} \leq 8$. The limited results here suggest the nominal stress at ultimate failure is not dependent on member thickness, but this warrants further investigation. Other things being equal, and provided the bolts are not too close together, a double-bolted fastener is appreciably stronger than a single-bolted fastener. However, the magnitude of the contact stresses does not decrease proportionally to the number of bolts used.

The present results, together with those of the other references cited, suggest that one should minimize the bolt clearance, $\frac{a}{R} \geq 10$ is probably adequate in many cases rather than the $\frac{a}{R} \geq 14$ of The National Design Specification for Wood Construction (National Forest Products Assoc 1986), and it can be important to strive toward equal loading among the bolts of a multiple-bolt connector. The practicality of using connectors having end-distance $\frac{a}{R} < 14$ also tends to be supported by recent results of Patton-Mallory (1988a).

The bolts were assumed to be rigid and hence nondeformable. However, the

full-scale physical testing of double-bolted three-member mechanical fasteners did consider members of different thicknesses, i.e., three-dimensional effects. If a bolt bends (such as in Fig. 1), the stresses in the wood will become three-dimensional and this could affect the type of failure. Rigorous pursuit of such a situation would necessitate a 3-D stress analysis, and a 3-D strength (failure) criterion. This implies the need for 3-D constitutive and strength wood properties, i.e., constitutive and strength in the thickness direction (in the bolt direction). To date most strength criteria have been applied only in the plane.

ACKNOWLEDGMENTS

REFERENCES

AGARWAL, B. L. 1980. Static strength prediction of bolted joint in composite material. AIAA J. 18(11):1371.

BODIG, J., AND B. J. M. FARQUHAR. 1988. Behavior of mechanical joints of wood at accelerated strain rates. Proc. Int'l Conf. Timber Engineering, Seattle, Sept., Vol. 2:455–464.

CHANG, F. K., R. A. SCOTT, AND G. S. SPRINGER. 1982. Strength of mechanically fastened composite joints. J. Composite Materials 16:470–494.

CHIANG, Y. J. 1983. Design of mechanical joints in composites. Ph.D. thesis (supervised by R. E. Rowlands), Department of Engineering Mechanics, University of Wisconsin, Madison, WI.

———, AND R. E. ROWLANDS. 1987. Fracture analysis of cracks emanting from a bolt-loaded hole in a composite. Presented at the 20th Midwest Mech. Conf., West Lafayette, IN (submitted for publication).

CRAMER, C. O. 1968. Load distribution in multiple-bolt tension joints. ASCE Jour. Struct. Div. 94: 1101–1117.

CREWS, J. H., AND R. A. NAIK. 1986. Combined bearing and bypass loading on a graphite/epoxy laminate. Composite Structures 6:21–40.

FAN, C. 1988. Behavior of bolted joints in timber structure and design formulae. Proc. Int'l. Conf. Timber Engineering, Seattle, Sept., Vol. 2:294–312.

GARBO, S. P., AND J. M. OGONOWSKI. 1981. Effect of variances and manufacturing tolerances on the design strength and life of mechanically fastened composite joints, vol. 1—Methodology, development and data evaluation. U.S. Air Force Report AFWAL-TR-81-3041, Flight Dynamics Laboratory, Wright-Patterson Air Force Base, OH.

HERRERA-FRANCO, P. J., AND G. L. CLOUD. 1986. Experimental analysis of multiple-hole arrays of composite material fasteners. Proc. Soc. Exp., New Orleans, June. Pp. 621–629.

HYER, M. W., AND D. LIU. 1984. Stresses in quasi-isotropic pin-loaded connectors using photoelasticity. Experimental Mechanics 24(3):48–53.

MCLAIN, T. E., AND S. THANGJITHAM. 1983. Bolted joint yield model. J. Structural Eng., ASCE 109(8):1820–1834.

NATIONAL FOREST PRODUCTS ASSOCIATION. 1986. National design specification for wood construction. Washington, D.C.

OPLINGER, D. W. 1976. Stress analysis of composite joints. Pages 405–452 in J. J. Burke and A. F. Gorum, eds. Adv. in Joining Technology. Army Mat'l Tech. Conf., Ser. 4, Sept.

———, AND K. R. GANDHI. 1974a. Analytical studies of structural performance in mechanically fastened fiber-reinforced plates. Proc. Army Symp. on Solid Mechanics: The role of mechanics in design—structural joints. Army Mat'ls. and Mech. Research Center, Watertown, MA, AMMC MS 74-8 (AD 786-543). Pp. 211–242.

———, AND ———. 1974b. Stresses in mechanically fastened orthotropic laminates. Proc. Conf. on Fibrous Mat'ls. in Flight Vehicle Design, Dayton, OH, May 21–24; also, Air Force Flight Dynamics Lab. Report AFFDL-TR-74-103, (AD-B000-135L). Pp. 811–842.

PATTON-MALLORY, M. 1988a. End distance effect comparing tensile and compression loads on bolted wood connections. Proc. Int'l Conf. Timber Eng'r., Seattle, Sept., Vol. 2:313–319.

———. 1988b. Use of acoustic emission in evaluating failure processes in wood products. Ibid. Pp. 596–600.

POST, D., AND T. F. MACLAUGHLIN. 1971. Strain analysis by moiré fringe multiplication. Experimental Mechanics 11(9):408–413.

PRABHAKAREN, R. 1982. Photoelastic investigation of bolted joints in composites. Composites 3: 253–256.

PYNER, G. R., AND F. L. MATTHEWS. 1979. Comparison of single- and multi-hole bolted joints in glass-fibre reinforced plastic. J Comp. Mat'ls. 13:232–239.

———, AND ———. 1980. A review of the strength of joints in fiber-reinforced plastics. Part 1: Mechanically fastened joints. Composites 11(3):155–???

RAHMAN, M. U. 1981. Stress and strength analysis of double-bolted mechanical joints in orthotropic materials. Ph.D. thesis (supervised by R. E. Rowlands), Department of Engineering Mechanics, University of Wisconsin–Madison, WI.

———, AND R. E. ROWLANDS. 1990. Finite-element analysis of tandom double-bolted mechanical joints of orthotropic members (in preparation).

———, ———, AND R. D. COOK. 1984. An iterative procedure for finite-element analysis of frictional contact problems. Computers & Structures 18(6):947–954.

ROWLANDS, R. E. 1985. Composite strength theories and their experimental correlation. Pages 71– 125 *in* A. Kelly and Y. Robotnov, eds. Handbook of Composites, vol. 3, North-Holland.

———, M. U. RAHMAN, T. L. WILKINSON, AND Y. J. CHIANG. 1982. Single- and multiple-bolted joints in composites. Composites July:273–280.

SABA, E. B., R. JANARDHANAM, AND D. T. YOUNG. 1988. The optimization of bolted timber joints. Proc. Int'l Conf. Timber Engineering, Seattle, Sept., Vol. 2:320–328.

SALINAS, J. J. 1988. Reliability bounds for bolted connections. Ibid. Pp. 143–148.

SOLTIS, A. L., AND T. L. WILKINSON. 1987. Timber bolted-connection design, building structures. Pages 205–220 *in* D. Sherman, ed. Proc. of Structures Congress '87 Related to Buildings, ASCE, Aug., Orlando, FL., also, USDA Forest Products Laboratory Technical Report FPL-GTR-54.

WALKER, G. R., AND N. K. MORROW. 1988. Transverse strength of bolted timber joints located near the ends of members. Proc. Int'l Conf. Timber Engineering, Seattle, Sept., Vol. 1:20–25.

WASZCZAK, J. P., AND T. A. CRUSE. 1971. Failure mode and strength predictions of anisotropic bolt bearing specimens. J Comp. Mat'l. July:421–425; also, AIAA Paper No. 71-354 (AIAA/ASME 12th Structural Dynamics and Materials Conference, Anaheim, CA, U.S.A., (April 1971).

———, AND ———. 1973. A synthesis procedure for mechanically fastened joints in advanced composite materials, vol. II. Air Force Mater. Lab. AFML-TR-73-vol. 2, Sept. (AD-771-795).

WILKINSON, T. L., AND R. E. ROWLANDS. 1981a. Analysis of mechanical joints in wood. Experimental Mechanics. 21(4):408–414.

——— AND ———. 1981b. Influence of elastic properties on the stresses in bolted joints in wood. Wood Science 14(1):15–22.

———, ———, AND R. D. COOK. 1981. An incremental finite-element determination of stresses around holes in wood plates, Computers & Structures 14(1–2):123–128.

WILSON, D. W., AND Y. TSUJIMOTO. 1986. On phenomenological failure criteria for composite bolted joint analysis. Composite Sci. Technol. 26(4):283–305.

WOOD HANDBOOK: WOOD AS AN ENGINEERING MATERIAL. 1974. U.S. Dept. of Agric., For. Prod. Lab., USDA Agric. Handbook 72.

YEN, S. W. 1978. Multirow joint fastener load investigation. Computers and Structures 9:481–488.